Structure and changing dynamics of a polythermal valley glacier on a centennial timescale: Midre Lovénbreen, Svalbard

Michael J. Hambrey,[1] Tavi Murray,[2] Neil F. Glasser,[1] Alun Hubbard,[3] Bryn Hubbard,[1] Graham Stuart,[4] Siri Hansen,[5] and Jack Kohler[6]

Received 29 January 2004; revised 28 October 2004; accepted 2 November 2004; published 10 February 2005.

[1] Most polythermal glaciers in Svalbard, other than those of surge type, have receded steadily since the early 20th century. Midre Lovénbreen, a slow-moving, 4-km-long valley glacier terminating on land, is a typical example, and its internal structures reflect changing dynamics over this period. The three-dimensional structural style of this glacier and the sequential development of structures have been determined from surface mapping, ground-penetrating radar, and numerical flow modeling. In order of formation the structures observed today at the glacier surface are (1) primary stratification that has become folded about flow-parallel axes; (2) axial plane longitudinal foliation associated with this folding; (3) several sets of intersecting crevasse traces; (4) arcuate upglacier-dipping fractures developed as part of a thrust complex near the snout; and (5) longitudinal splaying fractures in the snout area. The long-term evolution and dynamic significance of these structures can be ascertained from historical ground and aerial photographs. Modeling indicates that stratification and foliation continue to evolve today as a result of internal deformation, especially in zones of converging flow, where simple shear is most pronounced, but within the tongue are carried passively toward the snout. Crevasse traces appear to be no longer actively forming but are interpreted as relict structures when the ice was more dynamic and mostly wet based. The interpretation of arcuate fractures near the snout as thrusts is supported by the matching orientations of modeled strain ellipses, which illustrate the importance of longitudinal compression.

Citation: Hambrey, M. J., T. Murray, N. F. Glasser, A. Hubbard, B. Hubbard, G. Stuart, S. Hansen, and J. Kohler (2005), Structure and changing dynamics of a polythermal valley glacier on a centennial timescale: Midre Lovénbreen, Svalbard, *J. Geophys. Res.*, *110*, F01006, doi:10.1029/2004JF000128.

1. Introduction

[2] Glaciers of the maritime Arctic, such as those found in Svalbard, are known to be particularly susceptible to climatic change. The majority of nonsurge-type glaciers in this region have receded continuously since the Neoglacial maximum of around 1900 A.D. Of the numerous surge-type glaciers [*Dowdeswell et al.*, 1995], many have recorded at least one major advance in this period, but even these have receded substantially from their Neoglacial limits. Since it is recognized that climatic warming will be most marked in the polar regions, efforts are being made to assess the contribution of Arctic glaciers to sea level rise [e.g., *Dowdeswell et al.*, 1997; *Fleming et al.*, 1997; *Hagen et al.*, 2003]. This paper deals with an important aspect of glacier response to climate that has rarely been investigated: to determine how flow characteristics of a glacier change through time, especially as it recedes and thins in response to a warming climate.

[3] Few parts of the Arctic have glacier records that are long enough for these changes to be evaluated on longer than the decadal timescale. However, Midre Lovénbreen, a small polythermal valley glacier in Svalbard, has continuous mass balance records since 1967 [*Hagen and Liestøl*, 1990; *Lefauconnier and Hagen*, 1990]. There is also a series of aerial photographs taken by the Norsk Polarinstitutt dating back to 1936, and a number of historic ground-based photographs of the ice margin, the oldest dating from 1892. Thus, there is a unique data set for examining changes at the front and on the surface of this polythermal glacier.

[4] There has been some debate as to whether Midre Lovénbreen is a surge-type glacier. *Liestøl* [1988] argued, on the basis of it having a steep frontal cliff in the late 19th century, that it is a surge-type glacier. *Jiskoot et al.* [2000]

[1]Centre for Glaciology, Institute of Geography and Earth Sciences, University of Wales, Ceredigion, UK.
[2]School of Geography, University of Leeds, Leeds, UK.
[3]Department of Geography, University of Edinburgh, Edinburgh, UK.
[4]School of Earth Sciences, University of Leeds, Leeds, UK.
[5]Institute of Geography, University of Copenhagen, Copenhagen, Denmark.
[6]Norwegian Polar Institute, Polar Environmental Centre, Tromsø, Norway.

0148-0227/05/2004JF000128$09.00

found no evidence for surge-type behavior. A compromise view is that of *Hansen* [2003], who stated that the glacier may have been surging at its Neoglacial maximum, but has not subsequently done so.

[5] One way to determine the flow dynamics of a glacier is to map and evaluate its structural attributes, and many such studies have been undertaken on glaciers throughout the world (see *Hambrey and Lawson* [2000] for a review). In Svalbard, several structural investigations have been undertaken on surge-type glaciers, including Bakaninbreen [*Hambrey et al.*, 1996; *Murray et al.*, 1997, 2000], Hessbreen [*Hambrey and Dowdeswell*, 1997] and Kongsvegen [*Glasser et al.*, 1998; *Woodward et al.*, 2002]. Non-surge-type glacier studies are underrepresented. Nearly all previous structural studies have been based on contemporary aerial photography, and few have explored how structures have changed through time, except in the case of a handful of surge-type glaciers [*Lawson*, 1996].

[6] Most previous structural investigations of glaciers have relied entirely on surface mapping, and although this approach can be used to infer the internal structure, new technological developments, notably ground-penetrating radar, now allow the internal structure to be defined rigorously. This approach has already proved successful in defining thrusts during the termination of the recent surge of Bakaninbreen [*Murray et al.*, 1997] as well as ogives in Bas Glacier d'Arolla, a temperate valley glacier in the Swiss Alps [*Goodsell et al.*, 2002].

[7] In explaining the kinematic context in which glacier structures evolve, it is important to determine the cumulative strain field. Previously, cumulative strain has been determined (1) using finite element modeling in a vertical longitudinal profile through the Baffin Island Ice Cap [*Hooke and Hudleston*, 1978], and (2) by defining the flow field from an extensive network of velocity stakes on the Swiss Alpine glacier, Griesgletscher [*Hambrey and Milnes*, 1977]. In both cases, cumulative strain is represented as strain ellipses along flow lines through the glacier. More recently, thermomechanical flow modeling, has enabled derivation of the cumulative strain pattern for another Swiss Glacier, the Haut Glacier d'Arolla [*Hubbard and Hubbard*, 2000], a study which predates the preparation of a structural map [*Goodsell et al.*, 2005], but demonstrates the potential for evaluating a range of structures, such as foliation, folds and fractures.

[8] Building on the above research, the aims of this paper are to (1) describe the present-day structure of Midre Lovénbreen in 3-D on the basis of surface mapping and derivation of internal structure using the ground-penetrating radar technique, (2) use a flow-modeling analysis to gain insight into strain conditions under which certain structures form, and (3) evaluate how the dynamics of the glacier, derived from structural mapping, have changed over the past century, starting from the time that the glacier was at its maximal Neoglacial position, by historical photographs and through interpretation of relict structures.

2. Area of Investigation

[9] Midre Lovénbreen (78°52′N to 78°54′N, 11°57′E to 12°06′E) is a 4-km-long valley glacier, located in NW Spitsbergen, the largest island of the Svalbard archipelago (Figure 1). After White Glacier on Axel Heiberg Island, it is the most studied glacier in the High Arctic but no detailed structural analysis has previously been undertaken. Svalbard as a whole is 60% glacierized and is influenced by a maritime Arctic climate [*Hagen et al.*, 1993]. Midre Lovénbreen is typical of many small valley glaciers in the archipelago in having multiple accumulation basins (four cirques) feeding a narrow tongue (Figure 1). The equilibrium line altitude averages ~395 m above sea level (asl), and the accumulation area ratio of the glacier is 0.35 [*Björnsson et al.*, 1996]. Measured velocities on the centerline of the glacier in recent years have ranged from 4.4 to 7.3 m a^{-1} at the equilibrium line [*Björnsson et al.*, 1996; *Liestøl*, 1988].

[10] Midre Lovénbreen is known to be polythermal on the basis of radio echo soundings [*Björnsson et al.*, 1996]. Extensive areas of temperate ice up to 50 m thick lie beneath its accumulation area, but its terminus and margins are frozen to the bed. Further evidence of the polythermal character of the glacier is shown by the development of extensive areas of Aufeis (icings) immediately beyond the terminus, indicating that winter drainage persists even when the atmospheric temperatures are well below freezing [*Hagen and Sætrang*, 1991; *Ødegård et al.*, 1992; *Hagen et al.*, 1991; *Björnsson et al.*, 1996; *Hodson et al.*, 1997].

[11] Like most Svalbard glaciers of nonsurge type, Midre Lovénbreen has receded continuously since its maximum Neoglacial position of about 1890. The net mass balance of Midre Lovénbreen, derived from ground survey has been negative in most years since records began [*Lefauconnier and Hagen*, 1990; J. O. Hagen, personal communication, 2002], although the positive contribution of superimposed ice may have been underestimated [*Wadham and Nuttall*, 2003]. Historical photographs reveal that in 1892 the glacier snout had a vertical cliff [*Hamberg*, 1894]. Further ground photographs by *Isachsen* [1912] and *De Geer* [1930] indicate little change in the ice frontal position until 1923. Since that time, the snout profile has reduced to a low angle, in association with ~1 km of recession, an average rate of ~14 m a^{-1}.

[12] Glacier recession has revealed a complex sediment/landform association that can be linked to glacier structure and to the changing thermal regime of the glacier, comprising moraine mound complexes generated by englacial thrusting, diamicton sheets interpreted as basal till, trains of angular debris related to folding of supraglacial debris and stratified snow/ice about flow-parallel axes, and glaciofluvial deposits [*Hambrey et al.*, 1999; *Glasser and Hambrey*, 2001], together with small "concertina eskers" approximately 0.5 km from the glacier front [*Hansen*, 2003].

[13] To date, structural glaciological observations of non-surge-type glaciers in Svalbard have been limited to examining the relationship between medial moraines, folding and foliation. The snout of Midre Lovénbreen was included in these investigations [*Hambrey et al.*, 1997; *Hambrey and Glasser*, 2003], but not the whole glacier.

3. Data Acquisition and Analysis

[14] Structural mapping of the surface of Midre Lovénbreen was based on a 1995 aerial photograph of the Norsk Polarinstitutt. Additional maps were made from the 1948

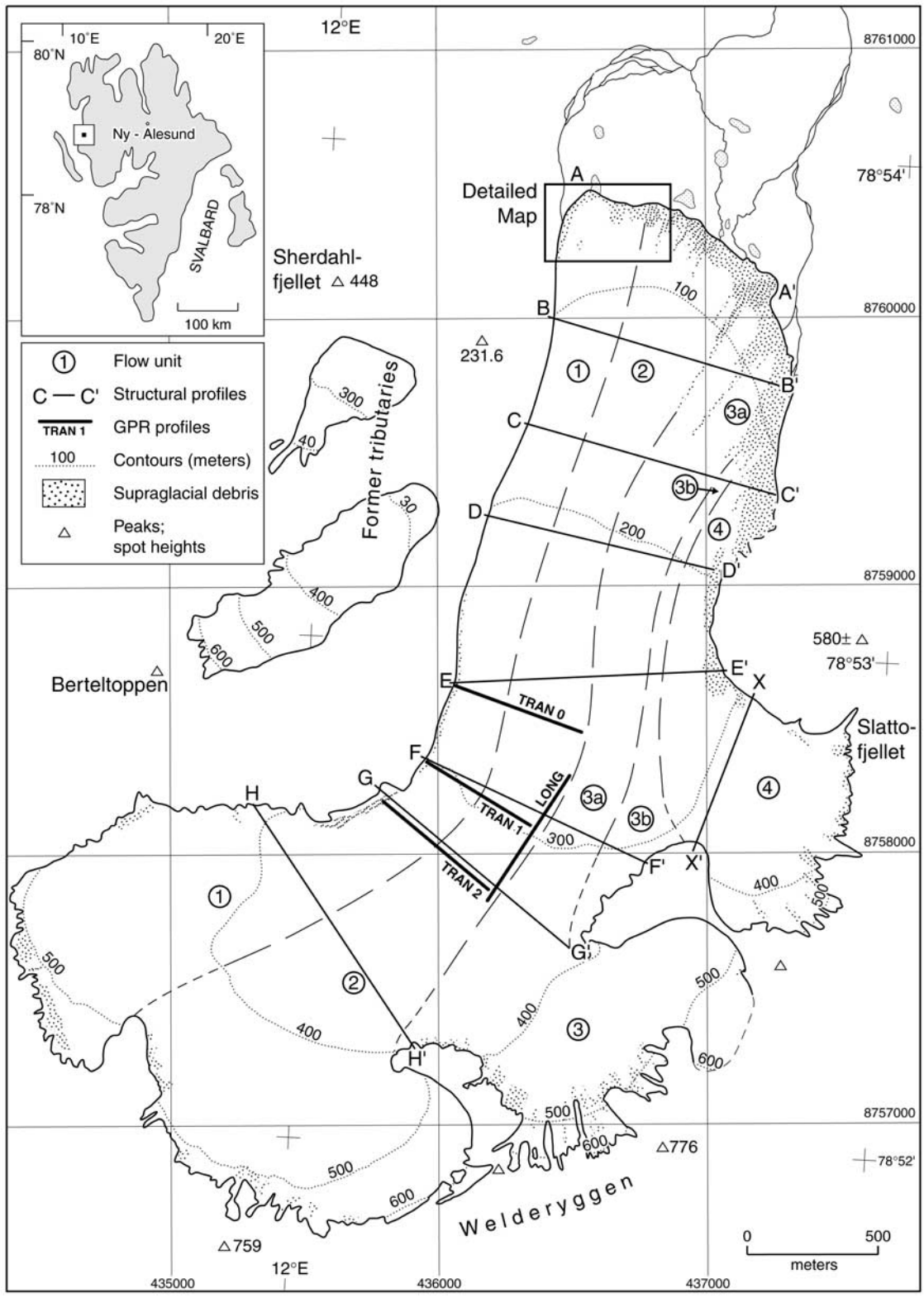

Figure 1. Flow unit map of Midre Lovénbreen and location of glacier within Svalbard. The topographic map is based on an orthophoto map prepared by *Hansen* [1999] from aerial photographs of the Norsk Polarinstitutt. Flow units are defined on the basis of ice structures observed on aerial photographs. The box at the snout refers to Figure 5.

and 1966 Norsk Polarinstitutt photographs to determine historical changes. Other photographic documentation used included an oblique Norsk Polarinstitutt aerial photograph from 1936 and that published in *Hamberg*'s [1894] description of the glacier terminus. Aerial photographs facilitate the discrimination of "flow units," the individual streams of ice, originating from separate cirques, which coalesce to form the tongue.

[15] Structures were verified in the field and mapped in 3-D on the ground using a compass/clinometer. Measurements were made on a series of transverse profiles up to the position of the late summer snow line in 1999 and 2000. Measurement intervals ranged from 25 m near the margins to 100 m in mid glacier. Data were collected for the following structures: longitudinal foliation, fold axes and various fracture systems. Orientation data are presented on Schmidt equal area lower-hemisphere projections. Where the number of data points is sufficient (typically >13 if well clustered), eigenvalues and eigenvectors have been calculated.

[16] Since structural mapping at the glacier-wide scale does not always demonstrate clearly relationships between different structures, one small area (approximately 350 by 250 m) near the snout was selected for detailed structural mapping during 1999. The map was constructed using an electronic distance measuring instrument, surveying along critical structures, notably medial moraines, longitudinal foliation and arcuate fractures, and recording 3-D orientation. Survey points were established on prominent debris ridges in the glacier forefield.

[17] Although the surface mapping gives strong clues as to the nature of the glacier structure in 3-D, accurate geometric detail at depth is gained from ground-penetrating radar. This is a sounding technique, and as such it provides better imaging of subhorizontal than subvertical structures. The technique proved especially good for defining large-scale folds. The radar surveys were undertaken in the zone of convergence of the flow units where strong folding was suspected during April 2000 (Figure 1), and in the detailed map area near the snout, where low-angle fractures were dominant, during July 2000. Whereas the sites in the zone of convergence yielded good quality structural information, the rough and wet surface and entrained debris during the summer survey scattered the signal at the snout site. Only data from the former sites were useful for structural analysis.

[18] Four common offset lines of over 3 km were acquired, together with common midpoint surveys for velocity, and therefore depth, control. Three lines crossed the glacier from west to east, denoted TRAN0 to TRAN2, and one line ran downglacier, denoted LONG (Figure 1). All data were collected with a Sensors and Software PulseEKKO 100 GPR, using 100 MHz antennae. For common offset surveys, an antennae separation of 2.0 m and a station spacing of 0.5 m were used. Given this station spacing, spatial aliasing occurs when the in-line dip of features exceeds $\sim 60^\circ$. Structures with greater dips are not correctly imaged and result in noise on the processed profile. Topographic data were collected using an electronic distant measurement instrument.

[19] Radar profiles (Figure 1) were processed using GRADIX 1.10 software (Interpex Ltd.) following despiking using Matlab to remove high-amplitude instrument-generated noise spikes. The processing was optimized to reveal the best level of detail of layered structures in the upper quarter of the glacier vertically using TRAN0, and then applied to all survey lines. Drift and time zero correction were applied, followed by a high-pass 5.6 MHz residual median filter (dewow) and band-pass filtering (trapezoidal filter set at 25-50-120-240 MHz) to remove noise. Coherent high-amplitude banding parallel to the ground surface is often present in radar data, especially at short reflection times. This was removed using the GRADIX background removal technique (window of 101 traces). Profiles were migrated using a frequency-wave number migration algorithm with a constant velocity of 0.168 m ns^{-1} (determined from velocity analysis of common midpoint surveys) and are displayed using a constant gain, which preserves reflection amplitudes. Sections in this paper are presented without surface topography, but the areas surveyed have a gradient of only a few degrees.

4. Contemporary Structural Glaciology of Midre Lovénbreen

4.1. Flow Units

[20] Interpretation of structures from aerial photographs indicates that the glacier consists of four major flow units, each originating from a cirque above 400 m asl (Figure 1). The flow unit boundaries were traced from the 1995 aerial photographs, being defined in the upper reaches of the glacier by a faint lineament on the snow or firn surface, then by strong longitudinal layering in the middle reaches and finally by medial moraines in the lower part of the glacier. The flow unit boundaries represent particle paths through the glacier. Confirmation was provided by checking rock types in the medial moraines at the snout (psammite, gneiss, phyllite and marble) against in situ lithologies in the headwalls. Each flow unit extends as far as the snout of the glacier, and most continue to flow actively, albeit at only a few meters per year. Flow unit 3 is divided into two, with 3b now severed from its source, and thus no longer contributing new mass to the glacier tongue. Two small cirques to the west of the glacier tongue are now disconnected from the main glacier by discontinuously exposed bedrock and a thick lateral moraine (Figure 2).

4.2. Surface Structures and Their Relationships With Debris

[21] The three-dimensional geometries of those structures exposed at the glacier surface were determined by measuring dip and direction of dip (1) along a profile close to and parallel to the snout (AA' in Figure 1), (2) on a further seven transverse profiles (BB' to HH'), although the upper two were only partially exposed; and (3) on a partially exposed transverse profile across flow unit 4. Five types of planar structures are recognizable on Midre Lovénbreen (Figure 3). They are described below in order of formation, as determined from cross-cutting relationships, and are labeled according to structural geological conventions. They are interpreted in section 8.1 in the context of their dynamic significance.

4.2.1. Continuous Layering (S_0)

[22] Irregular, but continuous layering is the earliest structure to appear in the glacier. It is visible in aerial

Figure 2. Vertical aerial photograph of Midre Lovénbreen, showing main structures in 1971 (see text and Table 1 for notation). Part of photograph S71 7057, published with permission of Norsk Polarinstitutt. The arrows indicate medial moraines defined by axes of folded debris layers parallel to continuous layering (foliation).

photographs from the superimposed ice limit downward, but disappears within 500 m of the snout (Figure 2). Viewed from the surface, this structure cannot be traced readily in the lower part of the glacier, but in the middle reaches it is clearly visible as layers that are continuous for tens of meters (Figure 3a). Dip is highly variable, ranging from near-horizontal to 70°. The structure has been folded on a large scale (wavelength of the order of tens of meters) about flow-parallel axes. Parasitic folds have axes that are readily measured and invariably have a gentle upglacier plunge (Figure 4). The folds (F_1) are of similar (Figure 3a) or chevron (Figure 3b) types, with thickened hinges and thinned limbs. Angular debris (sandy gravel, dominated by cobbles and boulders) forms discontinuous layers parallel to the ice layers, and becomes especially prominent in tightly folded zones at flow unit boundaries. Most of these folded debris layers emerge from point sources to form medial moraines within 1 km of the glacier snout.

4.2.2. Discontinuous Layering (S_1)

[23] Discontinuous layering of longitudinal orientation is evident through most of the glacier tongue, emerging from beneath the snow/slush line and extending nearly as far as the snout, although its strength is variable (Figures 3b and 4). The structure is pervasive except for two lozenge-shaped zones in flow units 1 and 2 where it is not visible (Figure 4 inset). It is also difficult to observe in the immediate vicinity of the snout. The layering is most pronounced at the glacier margins and at the flow unit boundaries 2/3 and 3/4. It is defined by intercalated layers of coarse bubbly and coarse clear ice, each individual layer being a few centimeters thick and traceable for little more than a meter. Discontinuous layering is weakest where it is dominated by coarse bubbly ice layers, several centimeters in thickness, and faint subcentimeter-thick clear ice layers. Near the western margin, this discontinuous layering contains mud, sand and disseminated gravel of variable shape, but with subangular and subrounded clasts dominant.

[24] The orientation of the discontinuous layering is consistent throughout the tongue (Figure 4). Dips range mainly from 80° to 90°, and the strike is parallel to flow unit boundaries and inferred particle paths. In places, particularly near flow unit boundaries, discontinuous layering intersects folded continuous layering, the two structures having an axial-planar relationship. However, the precise crystallographic relationship between folds and layering is unknown. Discontinuous layering, discordant with current flow unit boundaries, is evident in the severed ice remnant of flow unit 3b.

4.2.3. Multiple Fracture Sets (S_2)

[25] Few crevasses are evident at the surface of Midre Lovénbreen today; they are confined to the upper basins above the snow/superimposed ice line, and to the true left

Figure 3. Structures at the surface of Midre Lovénbreen. (a) Continuous layering, S_0, folded in similar fashion, interpreted as stratification; discontinuous longitudinal layering, S_1, interpreted as axial planar foliation is visible lower right; ice flow from top to bottom. (b) Continuous layering, S_0, folded in chevron fashion, interpreted as stratification; discontinuous longitudinal layering, S_1, interpreted as longitudinal foliation is strongly developed; shaft of ice axe is aligned parallel to the axis of F_1 folds; ice flow top to bottom. (c) Narrow crevasses and fractures interpreted as crevasse traces, S_2, in flow unit 4; ice flow left to right. (d) Arcuate fracture set, S_3, interpreted as a thrust sequence, seen in cross section at NW margin, with encircled persen fer scale; ice flow right to left. (e) Debris associated with thrusts near snout; note clearly defined debris layer where glacier surface has been cleaned above the ice axe head; ice flow top left to lower right.

margin between profiles G and F. None wider than 1 m was observed during the field program. Despite the lack of crevasses, there are numerous near-vertical fractures (Figure 3c). In cross section they typically consist of a few centimeters of coarse clear ice with a bubble "suture" down the middle; these are traceable across the ice surface for several tens of meters. Longitudinal layering is occasionally displaced sideways by a few centimeters across the fracture. A few geometrically related structures show rather thicker lens-shaped blue coarse clear ice bodies. Fractures occur in discrete sets, with individuals spaced a meter or more apart, slightly curving in plan view. Many fracture sets intersect one another; thus no clear geometrical pattern emerges from the measurements made.

4.2.4. Arcuate Fractures (S_3)

[26] Prominent sets of arcuate fractures distinct from crevasse traces are well developed within 0.5 km of the glacier snout and up to 1 km from the snout near the eastern

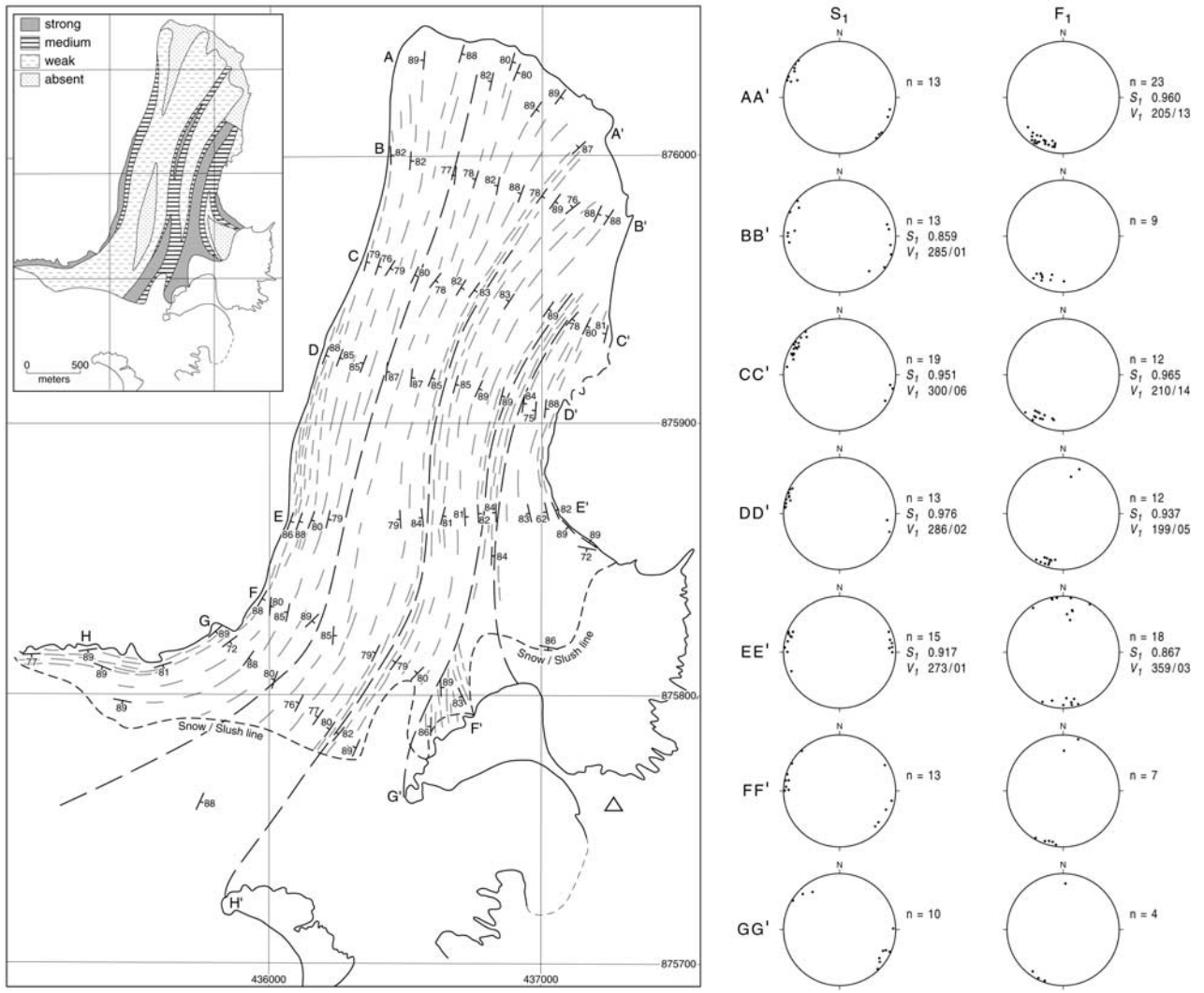

Figure 4. Map of foliation (S_1) with Schmidt equal area lower-hemisphere projections of poles to foliation and fold axes (F_1) on transverse profiles. Where data are sufficient, eigenvalues S_1 indicate strength of preferred orientation (italicized to differentiate from structural notation) and eigenvectors V_1 indicate preferred orientation of the structure. The inset (top left) illustrates qualitatively the strength of discontinuous layering (longitudinal foliation) in terms of visual impact based on ground observations and the 1995 aerial photographs.

margin. These are clearly seen in the 1995 and older aerial photographs (Figure 2). On the ground, a few can be observed as high as profile *EE′* on the west side of the glacier, 2 km from the snout. Arcuate fractures are well developed near the northwestern margin of the glacier, where they have been mapped to determine their geometry and cross-cutting relationships with each other and other structures (Figure 5). In general, they are subparallel to the ice front and are typically 50–100 m long. They cut across all structures except the longitudinal fractures, described below. The arcuate fractures are not exactly parallel to each other, and some intersect at a low angle. At their highest position on the glacier surface, they dip steeply up glacier (70°–80°), but their dip declines progressively toward the snout. From the way the arcuate fractures intersect other structures, they do not appear to be inherited from earlier structures, and clearly postdate the crevasse traces.

[27] Near the NW margin of the glacier, these features can be observed in cross section; here they leave the contact with the bed (composed of muddy sandy gravel) at an angle of about 20°–25° and rise asymptotically toward the ice surface, intersection with which gives rise to a slightly stepped profile (Figure 3d). The fractures themselves are defined by blue ice layers a few centimeters thick, along which disseminated mud is commonly found. These layers contrast with the coarse bubbly ice on either side. In cross section, as seen at the NW margin and in supraglacial streams, earlier structures, notably stratification, show meter-scale recumbent folding (F_2), with lower limbs truncated by the fracture. Visible displacements across the fracture are typically a few centimeters to a few decimeters (Figure 3d), the upglacier side overriding the lower, although many fractures show no displacements at all. Larger-scale displacements across some fractures may also

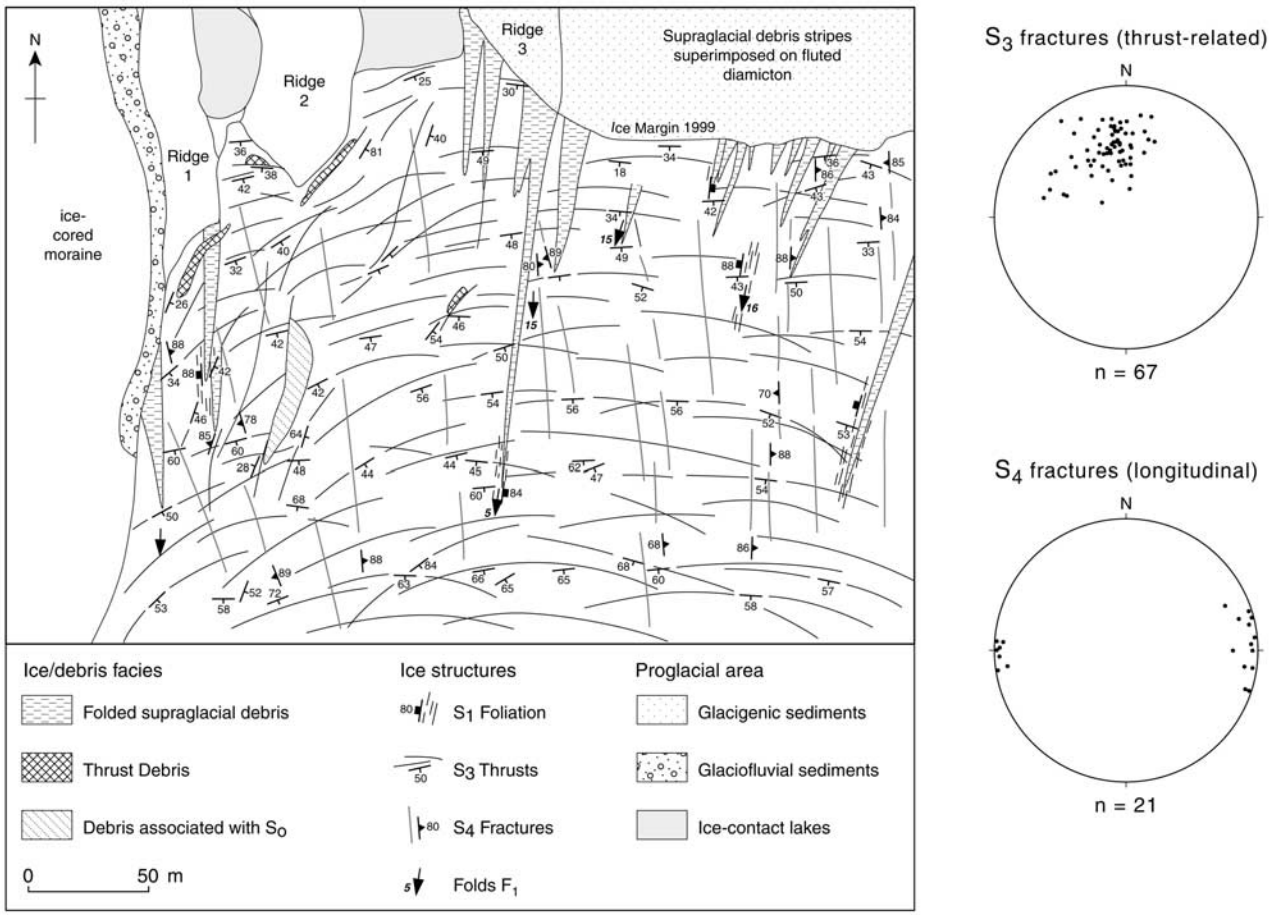

Figure 5. Electronic distance measuring survey of NW terminal region of Midre Lovénbreen, illustrating the relationships between thrust-related fractures (S_3), longitudinal foliation (S_1), fold axes (F_1), late longitudinal fractures (S_4), and debris cover. Partly based on map by *Glasser and Hambrey* [2001].

be present, but are difficult to recognize because distinct marker horizons are usually lacking.

[28] Within 100 or 200 m of the snout some of the arcuate fractures are associated with debris, either disseminated through the clear ice or forming discrete "slabs" of debris with interstitial ice up to 1 m thick (Figure 3e). This debris, when released at the ice surface, ranges from well-sorted sand and sandy gravel to diamicton, typical of glaciofluvial and basal glacial sediment respectively.

4.2.5. Longitudinal Splaying Fractures (S_4)

[29] The final planar structure observable is a slightly splaying set of faint longitudinal fractures in the lower 500 m of the glacier (Figure 5). They cannot be seen on the aerial photographs. They appear as closed cracks in the ice surface, tens of meters long, that appear to cut across arcuate fractures and discontinuous layering.

5. Internal Structure From Ground-Penetrating Radar

[30] Three transverse radar profiles were surveyed a short distance below the zone of convergence of flow units 1, 2 and 3a (Figure 1) to assess the internal geometry of the mapped structures. The dominant feature is a well-defined set of reflectors, arranged in a series of anticlines and synclines with wavelengths of ~50 to 100 m and amplitudes of ~5–40 m (Figure 6a). These reflectors are much stronger toward the western margin, and are completely absent from the eastern side of the glacier. They do not mirror the surface topography, but are truncated by it. The variation in amplitude and geometry between layers shows conclusively that few, if any, of the reflectors are internal multiples. The fold style is typically of the "similar" type, with thickened hinges and attenuated limbs, and there is some evidence of meter-scale parasitic folds on some anticlines (Figure 7). This structural style matches that of layering (S_0) and folds (F_1) mapped at the ice surface. However, some of the folds appear to be disharmonic, in that their axial planes are not continuous throughout the whole recorded depth in the sections (e.g., Figure 7, far right). There are also a number of discontinuities within the radar records which are probably unconformities (Figure 7). The overall structure indicates that the stratigraphically lowest (and therefore oldest) ice is exposed near the western margin.

[31] In a longitudinal profile (Figure 8), structures show a gently upglacier-dipping geometry, with only minor folding in the downglacier direction (e.g., at ~260 m along the

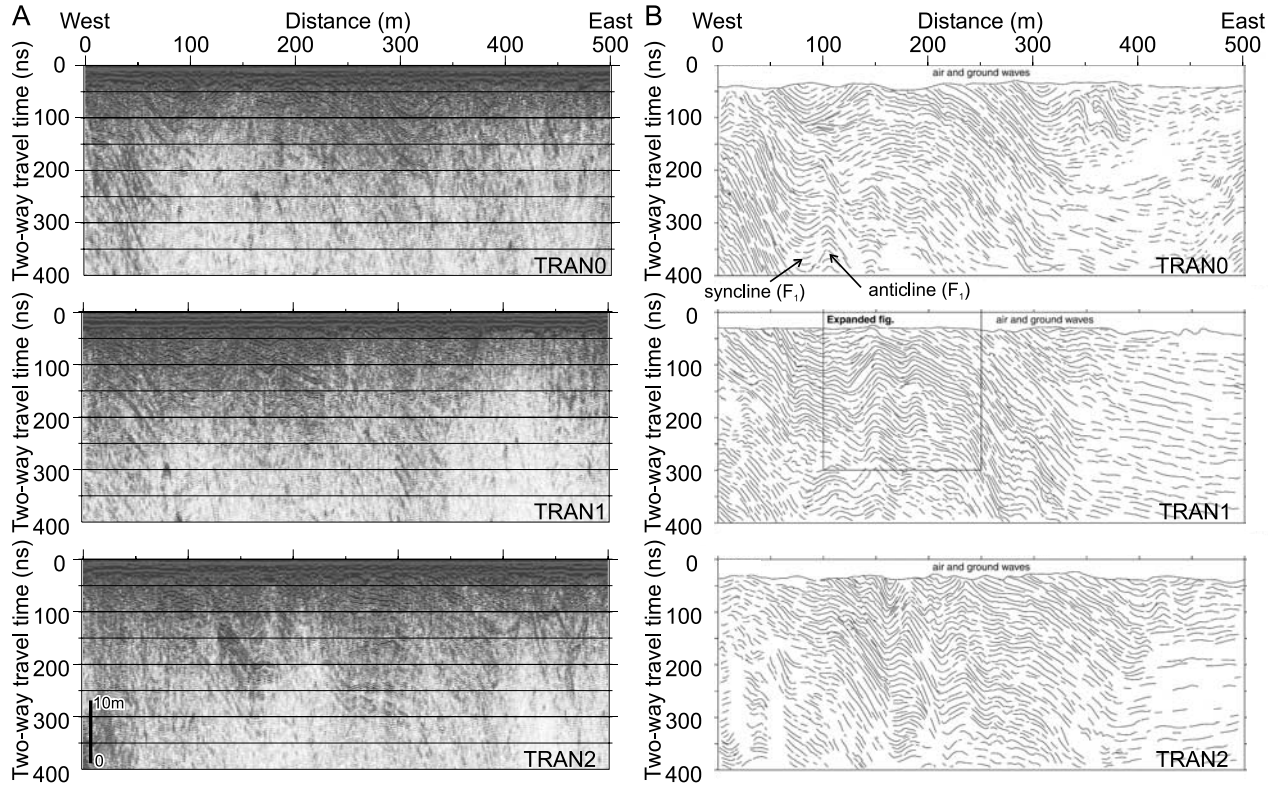

Figure 6. (a) Ground-penetrating radar profiles collected in spring 2000. Processing sequence is residual median filter 5.6 MHz, band-pass filter 25-50-120-240 MHz, set time zero, remove background using moving operator of 101 points, migration with fixed velocity 0.168 m/ns. Scale bar assumes a velocity of 0.168 m/ns. Ice flow into page. (b) Interpretation of radar profiles, showing cross sections through sedimentary stratification (S_0), folded by F_1, in the upper 20–30 m of the glacier on profiles below converged flow units. For location, see Figure 1.

profile LONG). Typically the features dip ~10 m in depth over length scales of ~100 m, and they become steeper downglacier.

[32] Other structures are less obvious. In certain zones (Figure 6b) there are numerous reflection hyperbolae, which have been successfully collapsed by the migration algorithm. These features are probably caused by englacial boulders or diffuse concentrations of debris. They could also result from small water bodies, although this is unlikely because they are surrounded by cold ice. In zones of tight folding, such as at flow unit boundaries (Figure 6b), the layering (S_0) is difficult to define, which is to be expected as the measured surface dip is too steep to be imaged by radar; these zones also coincide with strong, near-vertical longitudinal layering (S_1) as measured at the ice surface.

6. Structural Changes Since ~1890 A.D.

[33] In 1892, Midre Lovénbreen was at or near its Neoglacial maximum, and had a near-vertical terminal cliff (Figure 9) [*Hamberg*, 1894]. The height of this cliff is estimated from the moraine to be 20 to 35 m, but no measurements were recorded at the time. Midway along the snout, the structures dominating the cliff are gently upglacier-dipping planar structures. Although the photographs are unscaled, we estimate that these structures extend for more than 50 m. The lower one-third of the cliff was dominated by debris-rich or debris-streaked ice, the debris clearly emerging from several of these low-dip planar structures. The foot of the glacier cliff was dominated by a structurally controlled apron of boulder-bearing sediment emerging from a prominent planar structure dipping into the cliff at a low angle. The upper two-thirds of the cliff were

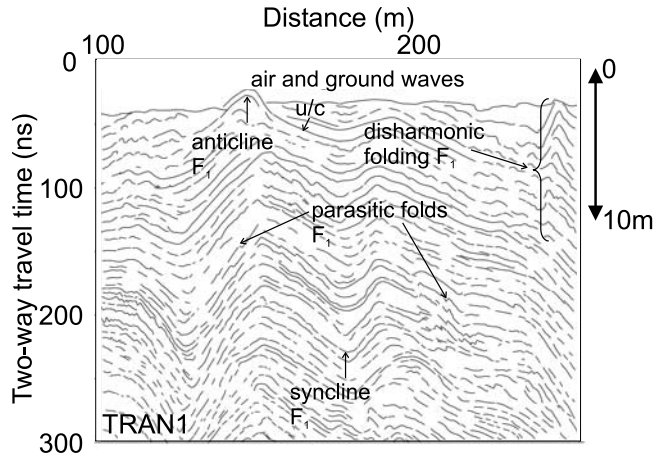

Figure 7. Interpretation of enlarged part of ground-penetrating radar profile TRAN 1 (A), illustrating details of fold style (F_1) and an unconformity (u/c) in S_0.

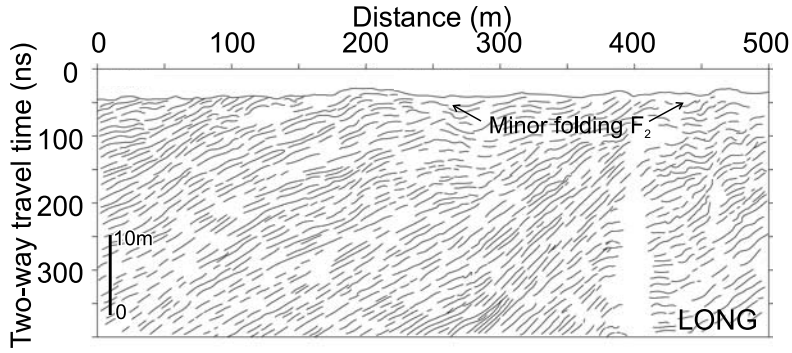

Figure 8. Interpretation of longitudinal ground-penetrating radar profile from Midre Lovenbreen, linking SE ends of transverse profiles and illustrating the generally upglacier geometry and gentle folding (F_2) of stratification (S_0). Ice flow is from left to right. Blank feature at 400 m along profile results from wire in the glacier. For location, see Figure 1.

mostly clean, but there were several additional discontinuous layers from which debris was emerging. From other early close-up photographs [*Hamberg*, 1894], the debris appears to be poorly sorted, with subrounded and subangular clasts dominant. From these observations, and through comparison with modern polythermal glaciers that are advancing (e.g., Trapridge Glacier, Yukon [*Clarke and Blake*, 1991] and Thompson Glacier, Axel Heiberg Island [*Hambrey and Lawson*, 2000], we infer that the structures were actively forming thrusts associated with basal debris. In terms of geometry, they compare well with the modern arcuate structures mapped in Figure 5, despite the latter being on a gently graded ice margin, over 1 km away from the 1892 position. It is not known how crevassed the glacier was at this stage, but from the abundance of crevasse traces today, it is likely that crevasses were well developed.

[34] The earliest oblique aerial photograph (Figure 10) shows that ice frontal recession had barely begun by 1936, but the ice margin was already much less steep. Structures are difficult to discern, but few crevasses are visible at the glacier surface, suggesting that the speed of the glacier had decreased.

[35] From the series of vertical aerial photographs available since 1948, three were selected for structural comparisons (Figure 11) in order to reflect changes in the second half of the 20th century. The dominant structures visible in the photos are stratification (S_0), foliation (S_1) and arcuate fractures (S_3) near the snout. Few crevasses or crevasse traces (S_3) are discernable, although the latter may be too faint to recognize. As the glacier has receded and narrowed, the stratification appears to have become more tightly folded, particularly near flow unit boundaries. In each of the years depicted, the arcuate fractures are located within ~1 km of the snout, even though there has been considerable recession. Since the tongue of the glacier is now largely frozen to the bed [*Björnsson et al.*, 1996], these arcuate fractures are probably no longer forming, but have become progressively exposed by ablation and thinning. The implication is that thrusting occurred throughout much of the tongue during the Neoglacial maximum, but that many thrusts failed to propagate to the surface. Over this same period, the glacier tongue has lost some of its accumulation area, with the severance of two former tributaries along the western margin from the main glacier. At current rates of

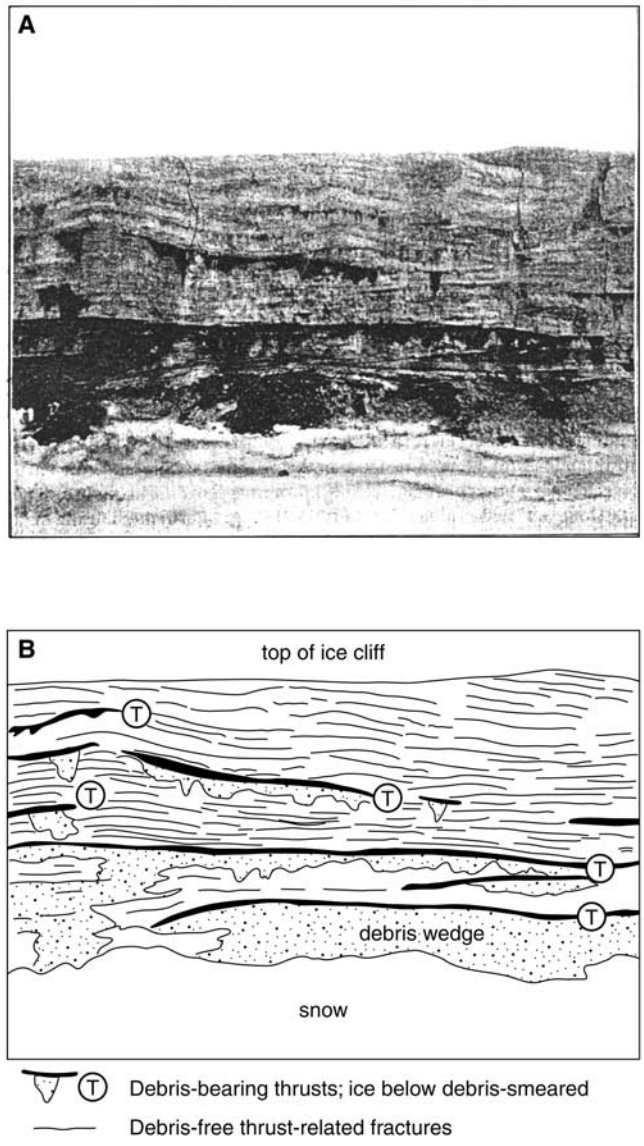

Figure 9. (a) The snout of Midre Lovénbreen from photograph by *Hamberg* [1894], with (b) our structural interpretation, focusing on thrust-related features. The ice cliff is 25–30 m high and represents a point midway along the snout of the glacier, i.e., normal to flow.

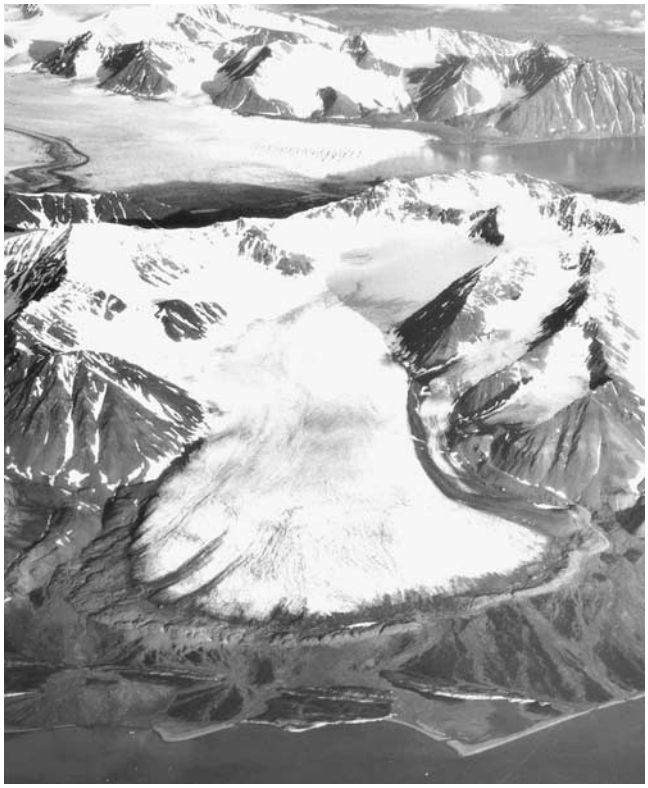

Figure 10. Oblique aerial photograph of Midre Lovénbreen in 1936, showing ice limit just inside Neoglacial moraine. Part of photograph S36 15 5 2, published with permission of Norsk Polarinstitutt.

recession and thinning of the tongue, it is also likely that the lowest (northernmost) of the eastern tributaries will also be severed in the near future.

7. Numerical Flow Modeling

[36] To understand the evolution and dynamic significance of structure in a glacier, the overall strain regime needs to be determined. In this case, thermomechanical flow modeling shows how circles (zero deformation) evolve into ellipses. The orientation and degree of elongation of the ellipses can therefore be compared with structures in order to discriminate simple shear, pure shear or extensional regimes. In this way, the evolution of penetrative structure can be tracked from start to finish.

7.1. Model Description and Validity

[37] As an independent assessment of the contemporary flow regime at Midre Lovénbreen and its impact on surface strain and structure, flow modeling was undertaken using a modified version of *Blatter*'s [1995] first-order algorithm for the solution of the grounded ice flow equations in three dimensions. The model was implicitly coupled to a thermal scheme and applied at a spatial resolution of 100 m in the horizontal and 2.5% of the local ice thickness, equating to 40 vertical layers, to yield the computed stress and strain fields. The model is steady state (i.e., time-independent), applied to the bed and surface geometry described for Midre Lovénbreen by *Rippin et al.* [2003]. The model has previously been successfully applied to Haut Glacier d'Arolla in Switzerland [*Hubbard et al.*, 1998; *Hubbard and Hubbard*, 2000], Taylor Glacier in Antarctica [*Hubbard et al.*, 2005] and Storglaciären in Sweden [*Albrecht et al.*, 2000; *Schneeberger et al.*, 2001]. The last of these is a polythermal glacier not dissimilar in size, structure and morphology to Midre Lovénbreen. However, up to now, this modeling approach has not yet been fully applied to structural interpretation. The model includes the first-order terms of the equations governing ice flow [*Blatter*, 1995], that is those lateral and longitudinal stress gradients which are pertinent to modeling valley glaciers, since significant compressive and tensile forces are induced both by local changes in glacier surface and bed slopes, and by basal and lateral friction.

[38] To calculate basal thermal conditions a thermal model was applied based on the heat supplied to the bed by geothermal flux, friction from ice deformation and sliding, and from the temperature gradient required to conduct that heat away. Frictional heating supplied to the bed (H) is calculated by

$$H = -\rho_i g \nabla(S) Q_i,$$

where $\nabla(S)$ is the ice surface slope, and Q_i is the ice discharge. Under an assumption that the bulk of differential motion, and thus heating, takes place at the lowest layers of the glacier, then frictional heating (H) and the geothermal heat flux (G) can be combined to yield the steady state temperature gradient required to maintain thermal equilibrium:

$$H + G = k \frac{\partial T}{\partial z},$$

where k is the thermal conductivity of ice and $\partial T/\partial z$ is the magnitude of the vertical temperature gradient. Vertical integration of this relation yields an expression for the internal and basal temperature of the glacier under an assumed surface-temperature boundary condition. A value of 55.0 mW m^{-2} was taken for the geothermal heat flux (G) and the surface temperature field was based on local meteorological measurements (J. Wadham, personal communication, 2003), which gave a mean annual temperature of -6.0°C at the terminus with a lapse rate of 0.0025°C m^{-1}. This thermal scheme was implicitly coupled with the first-order algorithm described above and used to replicate the present-day flow regime in two distinct stages: (1) by applying the model with zero basal sliding and comparing the computed surface strains with velocities based on repeat survey of a series of stakes up the glacier centerline (J. Wadham, personal communication, 2003), and (2) subsequently rerunning the model with a basal sliding distribution calculated by the residual between the modeled and observed surface velocity pattern and applied only to zones at the pressure melting point.

[39] This second model experiment yields a surface velocity pattern which corresponds well with the observed centerline measurements and, furthermore, is also consistent with the interpretation of radio echo sounding returns obtained by *Björnsson et al.* [1996], which indicate that the only significant zone of temperate basal ice is found

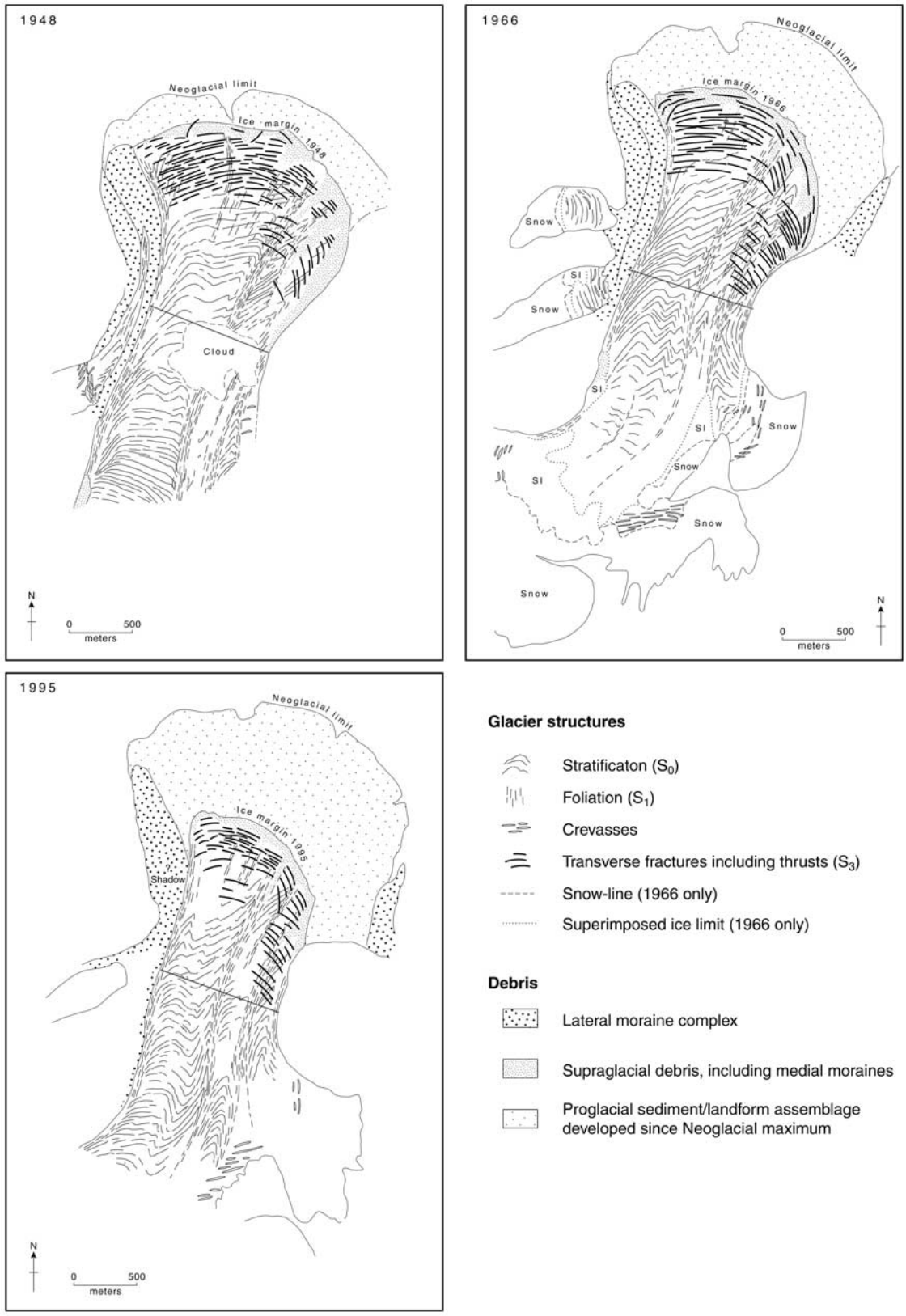

Figure 11. Surface structures of Midre Lovénbreen, based on vertical aerial photographs for 1948, 1966, and 1995. These maps are scaled to a common cross profile in midglacier (line indicated on each map) but are not corrected for edge distortion, which varies between photographs.

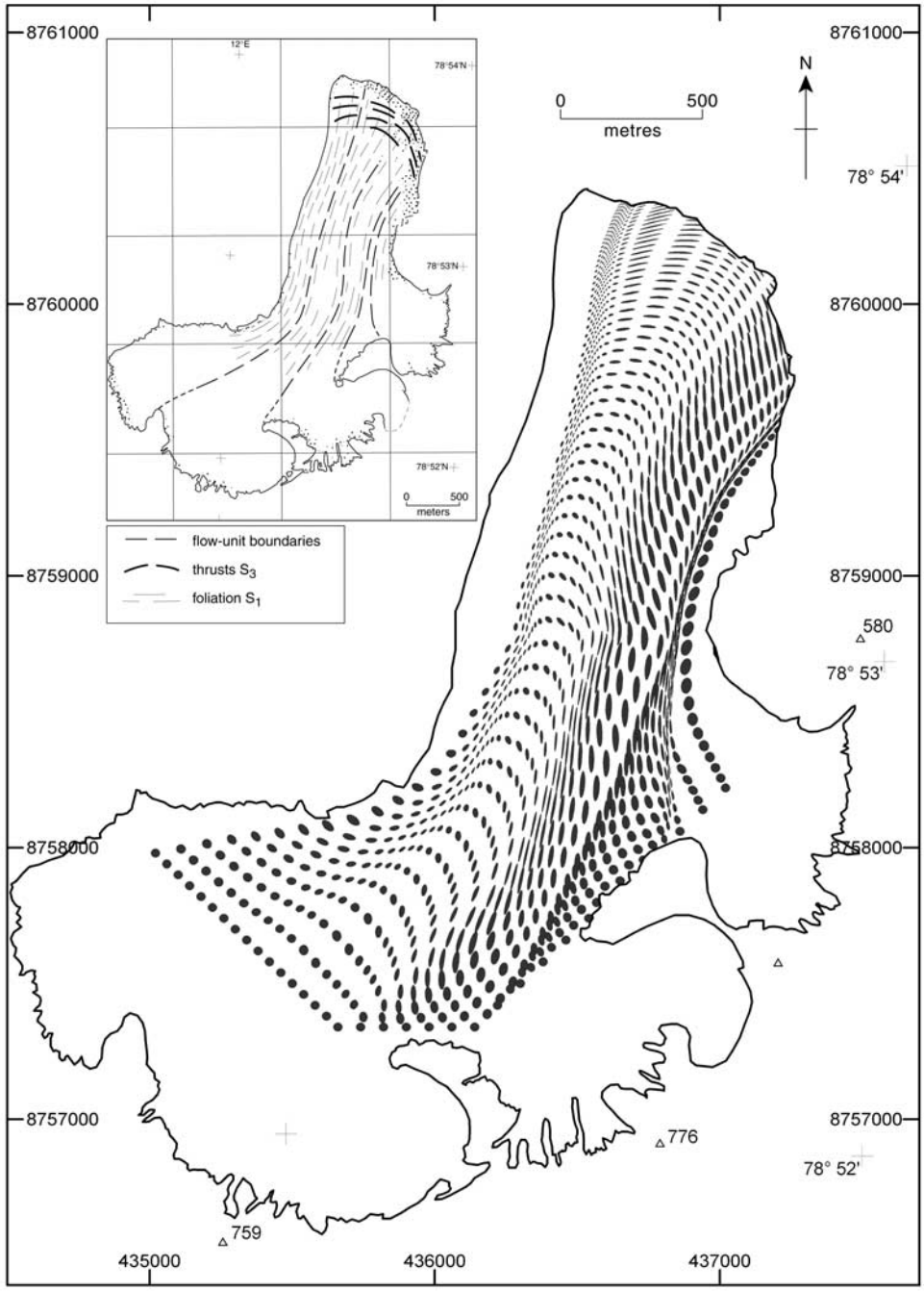

Figure 12. Results of numerical modeling experiment, illustrating how the strain regime evolves downglacier. Cumulative strain is expressed by the development of strain ellipses from circles. The inset shows flow units and generalized pattern of discontinuous layering (S_1) and arcuate fractures (S_3) from a 1995 aerial photograph, for comparison with strain-ellipse pattern.

across the upper accumulation area. This was precisely the footprint found to be at pressure melting point through thermomechanical modeling, and where an extensive zone of basal motion required specification for the second model experiment. Elsewhere along the centerline, the modeled internal deformation component accounts wholly for the observed surface velocity regime to within ± 1.0 m a^{-1}. It may be worth noting that the modeling indicates that the glacier is currently well out of balance with the current mass balance regime and that today's glacier geometry is more consistent with an equilibrium line altitude some 125–175 m lower than that of today. Thus continued rapid thinning and retreat is to be expected.

[40] The resulting three-dimensional modeled annual velocity pattern optimized against velocity measurements along the glacier centerline provides the basis for the present study, which utilizes a Lagrangian coordinate tracking algorithm to advect a series of cumulative strain circles downglacier (Figure 12). The circles are deposited on the glacier surface within the accumulation area, become par-

tially buried as they are advected downflow across the ELA and are subsequently reexposed at the surface by melting within the ablation zone. Although this scheme, strictly speaking, yields the englacial strain pattern, it is virtually identical to the resulting surface strain pattern since there is no appreciable difference between horizontal strain at the surface and the nominally buried depth of the circles across the ELA since ~90% of the strain is accounted for within the lower 25% of the ice column. The principal limitations of the model is that it assumes steady state conditions, yet we know that the glacier has shrunk and become less dynamic over the period that existing ice has resided within the glacier. However, although the magnitude of strain may have changed, the orientation pattern of the strain ellipses, determined by relative motion at the margins and between flow units, is likely to have changed little. Therefore we believe that the model, broadly, may be used to determine the strain field under which certain structures evolve.

7.2. Description of Strain-Ellipse Pattern

[41] Beginning with circles in the upper cirque basins, a complex pattern of strain ellipses develops as ice moves through the glacier (Figure 12), which consists of the following characteristics: (1) three main zones of strong cumulative strain associated with rotation into near longitudinal orientation where flow from each cirque basin converges; (2) a zone in midglacier with less intense strain indicating faster flow in midglacier and a slight tendency for strain ellipses with weak diagonal to longitudinal long axes to develop; and (3) with continued flow within the tongue (where the glacier has a consistent width, but broadening slightly at the snout), a new strain pattern is superimposed; ellipses become transverse to flow and are aligned in a single set of arcs of convex downglacier orientation, thus broadly mirroring the form of the snout. These key strain field characteristics are compared with structures and interpreted in section 8.2.

8. Discussion

8.1. Interpretation and Dynamic Significance of Contemporary Structures

8.1.1. Continuous Layering: Stratification (S_0)

[42] The continuous layering is interpreted as primary stratification. Its clear transition from layered snow and firn into glacier ice, and the continuity of layers bear out this interpretation. The initial character of stratified snow and firn has been described by *Wadham and Nuttall* [2003]. The original snow stratification at Midre Lovénbreen is heavily modified by melting and refreezing. A winter's accumulation typically consists of (1) a layer of high-density clear blue ice, representing refrozen slush at the base of the snowpack, overlain by (2) a layer of low-density "snow ice" that represents snow that was subjected to partial wetting and refreezing. In summer, especially near the equilibrium line, most of the snowpack is altered into superimposed ice by melting to slush and refreezing. Overall, superimposed ice contributes around 20% to the glacier-wide net balance on this glacier [*Wadham and Nuttall*, 2003]. As this heavily modified stratification moves down glacier, the resulting glacier ice is characterized by alternating layers of coarse bubbly ice, with numerous blue ice lenses, and coarse clear ice, the bubbly ice being dominant.

8.1.2. Folding of Stratification (F_1)

[43] Stratified ice next becomes folded, and then remains the dominant structure throughout most of the glacier tongue, where it is associated with axial planar foliation. Folding with near-vertical axial planes and flow-parallel axes affects the entire width of the glacier, although its strength is much greater where two flow units converge. This may not be so obvious at ground level, other than by the ubiquitous occurrence of minor folds, but is brought out dramatically in aerial photographs and ground-penetrating radar studies.

[44] Radar data support the presence of folded stratification and provide further information concerning its 3-D geometry. The geometry of the reflectors seen on profile LONG (Figure 8) is similar to that reported from a number of other Svalbard glaciers near the equilibrium line, with the upglacier dip reflecting a trend of increased accumulation or decreased ablation (J. Wadham, personal communication, 2003). In other words these researchers interpreted the structures to be currently forming stratification. However, at Midre Lovénbreen, the equilibrium line lay at about 265 m asl in 1990 and varied from 225 to 650 m asl during the period 1966 to 1991 [*Hagen et al.*, 1993]. Since the survey locations lie between 200 and 250 m asl (from Norsk Polarinstitutt 1:100 000 map A7, with contours dated 1956 and 1966) all lines lie within the ablation zone except during a very few exceptional years. It is therefore unlikely that these layers represent currently forming stratification. The geometry of the layers, combined with folding revealed in the cross-glacier radar profiles (Figures 6 and 7a), together with surface structures measured in the field and observed in aerial photographs (Figure 2) (Figure 13), suggests that this structure is stratification. However, this structure was formed upglacier of its current location and transported downglacier in a laterally compressive regime. The stratification was simultaneously folded about flow-parallel axes, and subsequently exposed by differential melting. Thus the transverse radar profiles lend strong support to the hypothesis that narrowing of the channel results in folding of the stratification to produce flow-parallel axes [*Hambrey et al.*, 1999]. It is also possible that there has been some downglacier longitudinal compression of the features, resulting in low-amplitude open folding (F_2), together with progressive steepening in a downglacier direction of the fold axes and stratification. The radar, therefore, is probably recording differences in the ice layering defined, before metamorphism, in the original snowpack by alternations of snow and superimposed ice.

[45] Although large-scale folding is well known from surge-type glaciers [e.g., *Post and LaChapelle*, 1971], reports from most nonsurge-type valley glaciers describe minor folding, but appear not to recognize large-scale upright folding [e.g., *Hambrey and Müller*, 1978]. Yet, visual inspection of aerial photographs indicates that many glaciers in Svalbard show evidence of large-scale upright folding. Thus although subtle, it may be more prevalent generally in valley glaciers than previously determined.

8.1.3. Discontinuous Layering: Foliation (S_1)

[46] Discontinuous layering in glaciers is usually referred to as foliation, a structure which is the product of ductile

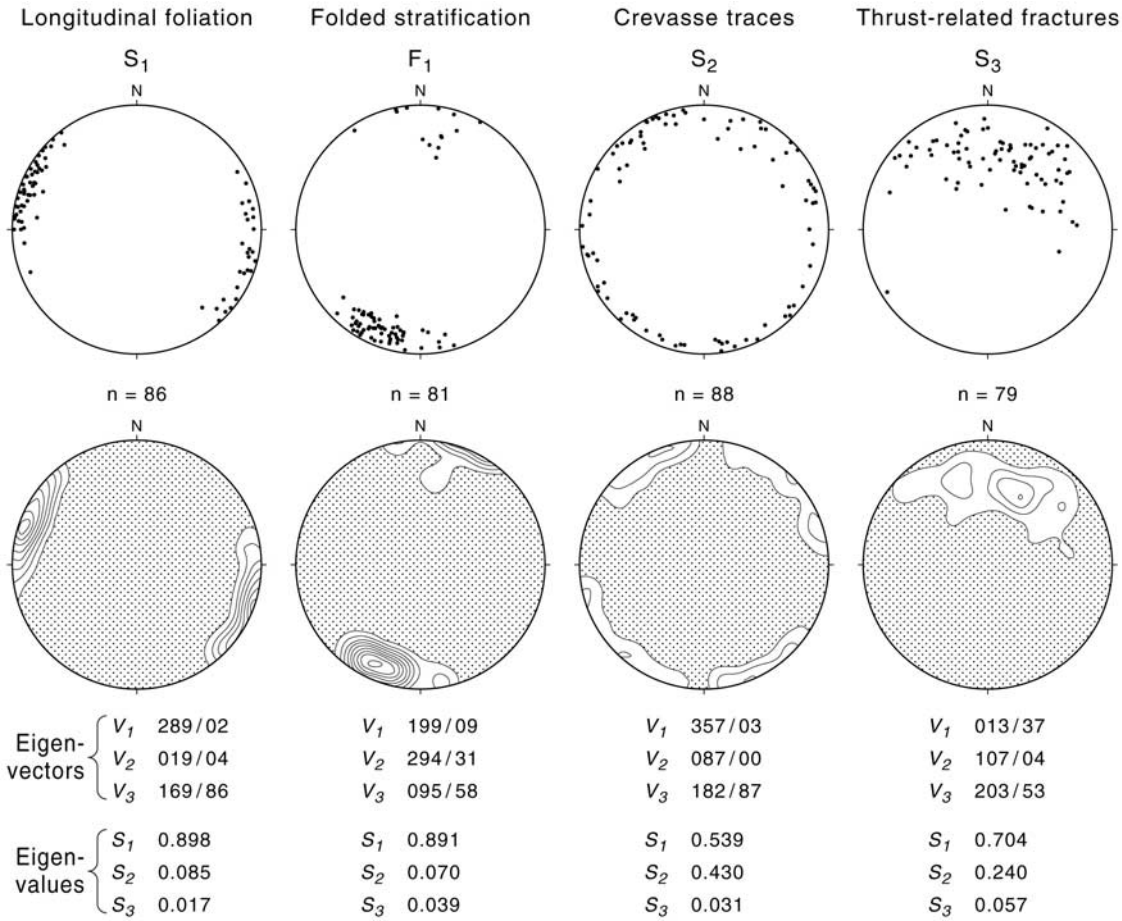

Figure 13. Cumulative structural data for poles to foliation (S_1), folds (F_1), poles to crevasse traces (S_2), and poles to arcuate thrust-related fractures (S_3) in the straight section of glacier from profiles AA' to FF' (Figure 1). Eigenvectors ($V_{1\text{-}3}$) and eigenvalues ($S_{1\text{-}3}$) are shown for each structure, italicized to distinguish from structural notation. Stereograms are Schmidt lower-hemisphere equal area projections with a contour interval of 2% per 1% of area.

deformation. Foliation has several origins, the most common being the result of the effect of pure or simple shear on preexisting structural inhomogeneities such as stratification and crevasse traces [*Hooke and Hudleston*, 1978], or transposition of earlier layering [*Hambrey*, 1977]. Neither mechanism applies to Midre Lovénbreen, as foliation cuts across stratification in a geometrically similar manner to slaty cleavage in folded sedimentary rocks. Longitudinal foliation pervades much of the width of the glacier (Figure 4), but is strongest at flow unit boundaries, a feature characteristic of many glaciers irrespective of size [*Allen et al.*, 1960; *Meier*, 1960; *Hambrey and Müller*, 1978; *Hambrey and Dowdeswell*, 1997].

8.1.4. Fracture Sets: Crevasse Traces (S_2)

[47] Crevasse traces (S_2) are a feature of most glaciers [*Hambrey and Lawson*, 2000], but can normally be linked to open crevasse fields, where they occur below, between or extending to the side, of crevasses. As noted above, very few open crevasses currently exist on Midre Lovénbreen; they are narrow and limited to the upper basins. By analogy with other glaciers, the fracture sets at Midre Lovénbreen are interpreted as crevasse traces. These are formed by two main processes: (1) as tensional veins whereby new ice crystals grow parallel to the principal extending strain rate tensor at the same rate of opening of the fractures, and (2) by freezing of water in crevasses to give thick blue ice layers. The former are analogous to tensional veins in deformed rocks [*Durney and Ramsay*, 1973; *Hambrey and Milnes*, 1977]. The presence of so many crevasse traces suggests that the glacier in the past was much more heavily crevassed, and that these relict features are now being transported passively downglacier.

8.1.5. Arcuate Fractures: Thrusts (S_3)

[48] The interpretation of the arcuate structures (S_3) that occur near the snout of Midre Lovénbreen is more problematic. One hypothesis is that they are thrusts. Thrusting has been recognized in many glaciers, and several criteria have been listed to facilitate their identification [*Hambrey et al.*, 1999]. Thrusts are common in many polythermal glaciers and, in Svalbard, have been described especially from the surge-type glacier Bakaninbreen, where upward displacement along the fracture has been demonstrated [*Murray et al.*, 2000], Hessbreen [*Hambrey and Dowdeswell*, 1997], and Kongsvegen [*Glasser et al.*, 1998]. Elsewhere in the Arctic, polythermal Storglaciären in northern Sweden, which is broadly similar morphologically to Midre Lovénbreen, has similar debris-laden arcuate fractures. These fractures have been interpreted as either shear zones [*Janssen et al.*, 2000]

or a combination of recumbent folding and thrusting [*Glasser et al.*, 2003]. However, alternative explanations exist for debris-laden examples of arcuate fractures, including rotation of basal crevasse fillings [*Woodward et al.*, 2002].

[49] The weight of evidence at Midre Lovénbreen suggests that these arcuate fractures are thrust faults, although it is difficult to demonstrate large displacements along these features because of the lack of distinctive marker horizons. Nevertheless, substantial amounts of debris of basal origin are found at the glacier surface, so the inference is that substantial (tens of meters) of uplift must have taken place along some fractures, but many other fractures may have had minimal displacement. In support of thrusting, several specific features stand out: (1) entrainment of basal and subglacial debris along arcuate fractures that reach the ice surface, including glaciofluvial material that would be difficult to squeeze into basal crevasses; (2) the incorporation near the snout of a frozen block of sand and gravel in which primary sedimentary structures (cross bedding and planar lamination) are preserved; (3) at the true left margin the fractures are connected to the bed, and allow muddy basal water to reach the surface; (4) a few recognizable displacements of several centimeters to half a meter have been measured in vertical cross sections, most obviously along the true left-hand margin near the snout and in association with recumbent folding (F_3) observed in the channel walls of downglacier-flowing streams.

[50] Since many of these arcuate fractures show no visible displacement, one has to assume that only a small proportion of them underwent differential slip. The apparent thrusts near at the true left margin today appear to rise up from a frozen bed (Figure 3d), but the sedimentological characteristics of the underlying sediment indicates that, in the past, the bed was wet [*Glasser and Hambrey*, 2001]. Therefore these fractures are probably no longer active, but may have formed when the ice was thicker, sliding over its bed and much more dynamic, probably at the time of its last advance.

8.1.6. Longitudinal Fracture Sets (S_4)

[51] These longitudinal splaying fractures probably reflect slight extension approximately orthogonal to the flow direction where the snout of the glacier emerges from the confines of the valley. Their impact on the visual appearance of the ice is minimal.

8.1.7. Contemporary Structural Evolution

[52] Contemporary structures are folded stratification and the associated axial planar foliation, while crevasses (or crevasse traces) and thrusts are not. Apart from the longitudinal fractures near the snout and a few crevasses in the upper basins, brittle fracture was therefore largely limited to the Neoglacial maximum phase when the glacier was at its most dynamic.

8.1.8. Evidence for Past Surge Behavior?

[53] Midre Lovénbreen has a suite of structures that broadly resembles those of other small valley glaciers in Svalbard that do not surge, notably straight moraines and undistorted longitudinal foliation (S_1) (Figure 4). *Liestøl* [1988] argued that Midre Lovénbreen was a surge-type glacier solely on the basis of its steep frontal cliff. In the Svalbard glacier inventory, Midre Lovénbreen is also classified as a surge-type glacier [*Hagen et al.*, 1993]. One of the present authors has suggested on the basis of a "concertina esker" on the modern glacier forefield that, although the glacier has not surged since the Neoglacial maximum, it may have done so prior to that date [*Hansen*, 2003]. On the other hand, *Jiskoot et al.* [2000] suggested that Midre Lovénbreen should be reclassified as nonsurge-type based on its very poor fit to statistical models of surge-type glaciers. The current structural glaciological work provides no evidence in favor of past surging behavior. The usual attributes of surge-type glaciers in their quiescent state are folded (looped) moraines, ice stagnation features and potholes, none of which are present on Midre Lovénbreen. The consistent trend of the foliation indicates that the individual flow units have responded to changes in mass balance uniformly for the time (probably a few hundred years) that ice has traveled through the glacier.

8.2. Relation of Structures to Cumulative Strain Geometry

[54] Flow units (Figure 1), defined by structure (longitudinal foliation, S_1) coincide with zones where ellipses have rotated into a near-longitudinal orientation, suggestive of a simple shear regime (Figure 12). Cumulative deformation is most pronounced at the zone of convergence, there being little evidence of continuing simple shear in the tongue. Specifically, flow unit boundaries 1/2, 2/3a and 3b/4 are clearly defined by the ellipse pattern. This pattern of rotation of strain ellipses toward parallelism with longitudinal foliation has been demonstrated using velocity/flow line maps previously on Griesgletscher, Switzerland [*Hambrey and Milnes*, 1977]. A similarly complex strain regime for another small valley glacier with multiple accumulation basins, the Bas Glacier d'Arolla in Switzerland, using the present modeling technique, has been derived by *Hubbard and Hubbard* [2000]. Foliation is weak where the sublongitudinal strain ellipses are not pronounced. There is an anomalous pattern between flow units 3a and 3b. The reasons for this are probably (1) poor structural resolution because of discontinuous snow and superimposed ice cover; (2) insufficient data to model the complex subglacial topography in this area; or (3) change in dynamics and partial severance of the source area as the glacier has thinned. The fold pattern is best developed in flow unit 2. The pattern of ellipses broadly mirrors the convex downglacier arcs that define the surface outcrops of the gently dipping structure, but the actual structural details are more complex.

[55] The fractures at the snout (S_3) are interpreted as thrusts, although they probably are no longer actively forming, because frozen bed conditions now apply here. The ellipse pattern here, with long axes parallel to ice margin, has taken over from longitudinally orientated ellipses. The overall pattern mirrors the orientation of fractures, with the short axis of ellipse (maximum compression) normal to the trend of the fractures. If this ellipse pattern can be extrapolated back in time, as seems reasonable, then the fractures are a clear indication of a longitudinal compressive regime that produces thrusts.

8.3. Sequential Development of Structures

[56] Five planar structures and two phases of folding characterize the tongue of Midre Lovénbreen (Table 1). Grouping all sets of structural data on profiles AA' to FF'

Table 1. Structures in Midre Lovenbreen and Their State of Evolution

Structure Description	Structure Interpretation	Symbol	Actively Forming?
Continuous layering	stratification	S_0	yes
Discontinuous layering	longitudinal foliation resulting from simple/pure shear	S_1	yes
Multiple fracture sets	crevasse traces related to period of extensive crevassing	S_2	no
Arcuate fractures; some associated with basal debris	thrust-related fractures propagating from bed	S_3	probably no
Longitudinal splaying fractures	minor extensional fractures associated with glacier widening	S_4	yes
Medium- to high-amplitude folding	folding of stratification with axes parallel to flow	F_1	yes
Transverse low-amplitude folding observed only in longitudinal radar profile	folding associated with initial longitudinal compression in glacier tongue	F_2	yes
Transverse recumbent folding	folding associated with thrusting when glacier more active	F_3	probably no

(the straight section of the glacier tongue where flow direction is consistent) indicates the nature of the relationships between structures (Figure 13).

[57] The relationship between folded stratification and foliation is clearly indicated in the first two columns of Figure 13. Both structures show a strong preferred orientation with S_1 eigenvalues approaching 0.9. Poles to foliation plot at right angles to F_1 fold axes (compare eigenvectors V_1 = 289 and 199°), indicating that the foliation plane defines the axial plane of the folds. The consistency of the relationships between stratification, folds and longitudinal foliation implies that they are associated with a common deformation regime. This relationship between folds and foliation is also a feature of several other glaciers in the vicinity of Midre Lovénbreen [*Hambrey and Glasser*, 2003]. The location for the development of these structures is most likely to be in the zone of converging flow units and thickening, where ice from the four accumulation basins feeds into the narrow tongue. Following the principles of structural geology [e.g., *Ramsay and Huber*, 1983], it is evident that folding accompanied by simple shear occurs in response to layer-parallel shortening of stratification. The process results in the suite of similar folds with wavelengths on the 100 m scale together with meter-scale parasitic folds. As the ice is subject to ablation downglacier, progressively deeper structures are exposed at the glacier surface. Eventually, near the snout, debris derived from the headwalls (and forming part of the stratified sequence) is reexposed. The geometry of these debris layers reflects tight folding, and the fold axes are parallel to the moraine crests and to the longitudinal foliation, which in turn are probably parallel to the ice flow direction.

[58] The plot of S_2 fractures, crevasse traces, is much more scattered, characterized by no clear pattern other than a bimodal distribution of steep transverse fractures (Figure 13, column 3). The presence of crevasse traces suggests formation in an extensional flow regime that is no longer evident in the glacier tongue. However, the presence of intersecting fracture sets and evidence of rotation indicate the cumulative effects of temporal and spatial variations in the flow regime of the glacier.

[59] Thrust-related fractures, S_3, show a moderately strong (eigenvalue S_1 = 0.7) girdle fabric, very close to being exactly transverse to flow (V_1 = 013°) (Figure 13, column 4). This data set embraces the full range of dips of this structure and represents what would be expected under a regime of longitudinal compression.

[60] From a combination of surface measurements, radar profiles and flow modeling, we can now define how the structure of a parcel of ice evolved in relation to cumulative strain as it moved from the accumulation basin through to the glacier snout along the flow centerline. At the start of its journey, this parcel of ice can be conveniently depicted as a sphere. The associated structure was ''layer cake'' stratification (S_0) of firn and ice. As it entered the narrow tongue, the sphere was deformed into an ellipsoid, elongated parallel to ice flow. The stratification was folded (F_1) about flow-parallel, near-horizontal axes, which were also parallel to the long axis of the cumulative strain ellipsoid. Axial plane foliation was formed simultaneously with the folding. Fracturing under an extensional regime then affected the parcel of ice, giving rise to crevasse traces (S_2) which intersect both S_0 and S_1. However, the cumulative strain ellipsoid was not significantly modified through this phase, and the substantial accumulation of strain associated with folding and foliation development was not reversed. Toward the snout, the ellipsoid, orientated parallel to flow, was subject to longitudinal compression in association with the development of thrusts (S_3). However, this too was insufficient to undo the strain associated with the development of S_1 and F_1. The final structure (S_4) also had little effect on the cumulative strain experienced by the parcel of ice. Thus overall, the zone where the parcel of ice was most strongly deformed was where ice from multiple basins converged into the narrow tongue.

8.4. Dynamic Response to Climatic Warming

[61] Midre Lovénbreen has seen significant changes since the earliest recorded observations in the 1890s which coincided with the Neoglacial maximum. The glacier has receded approximately 1 km, or ~20% of its original length. It has also lost an estimated 25% of its mass [*Hansen*, 1999]. Changes in mass were reflected mainly in thinning of the snout in the first third of the 20th century (Figure 10), then by steady recession of the snout thereafter (Figure 11). Recent decades have seen the severance of two of its tributaries, originating from cirques above the western margin. This separation followed ice stagnation beneath a supraglacial debris mantle, now represented by the left lateral ice-cored moraine. Four basins continue to supply ice to the tongue, but at low velocities (<10 m a^{-1}).

[62] These changes in morphology have been accompanied by decreased dynamic activity. Photographs from 1892 suggest active thrusting in the frontal cliff, while the abundance of crevasse traces suggests that at some time in the past the glacier was heavily crevassed. By 1936, the glacier front was no longer marked by a cliff, had receded slightly, and revealed a near-absence of crevasses

(Figure 10). This pattern of recession is typical of most land-based glaciers in Svalbard.

[63] Complementary sedimentological investigations in the proglacial area provide further manifestation of the changing dynamics of the glacier through the 20th century [*Glasser and Hambrey*, 2001]. Basal till from a wet-based glacier and deposition of a thrust-moraine complex of mixed facies were the main products when the glacier was at its advanced state. Deposition near the snout today reveals a frozen substrate with no evidence of sliding or subglacial deformation; the bulk of sediment released from the glacier is supraglacial. Although reworking of sediment by numerous small supraglacial streams and one subglacial channel is taking place, large areas of basal till in the proglacial area are simply receiving a drape of angular debris that originates from the structurally controlled medial moraines within the glacier.

[64] It follows that the major reduction in dynamic activity took place in the early part of the 20th century when the major loss of mass over the tongue was recorded. As the ice thinned, so the winter cold wave was able to penetrate the bed and freeze the substrate, effectively ending subglacial deposition in the terminal region. However, the thicker upper reaches of the glacier remain wet based [*Björnsson et al.*, 1996; *Rippin et al.*, 2003].

[65] In view of the almost consistently negative mass balances recorded over the last 35 years (two positive and five neutral years being exceptions), rapid thinning and recession of the tongue will continue. More specifically, unless mass balance returns to a positive state, it is likely that flow units 3a and 4 (Figure 1) will become progressively less able to contribute ice to the glacier tongue. It is instructive to make comparisons with neighboring austre Brøggerbreen, which has a similar altitudinal range, but is thinner, has a snout of even lower gradient, and is believed to be mostly cold throughout [*Björnsson et al.*, 1996]. Midre Lovénbreen is thus likely to follow the same cooling trend, and is expected to become cold throughout in due course.

8.5. Use of Structural Glaciology in Evaluating Changing Glacier Dynamics

[66] This study of the structure of a small valley glacier, using structural geological, geophysical and modeling techniques, has demonstrated how past changes in glacier flow and thermal regime may be determined. The timescale relevant to such studies in Svalbard is of the order of a century, i.e., since the Neoglacial maximum. We suggest that similar structural glaciological studies in remote areas, from where historical information is absent, would also yield valuable results. This approach is appropriate for timescales equivalent to the residence time of ice within a glacier, probably a few decades for temperate alpine glaciers, to several thousand years for the large individual drainage basins of the Greenland and Antarctic ice sheets.

9. Conclusions

[67] Midre Lovénbreen is a small slow-moving valley glacier terminating on land in northern Spitsbergen, and its structures reflect changing dynamics over the past century. In common with other polythermal glaciers in Svalbard, unless they are of surge type, Midre Lovénbreen has receded at a variable rate since the Neoglacial maximum near the end of the 19th century. Several conclusions may be drawn from this study of structures and associated phenomena in Midre Lovénbreen.

[68] 1. The style and sequential development of structures in Midre Lovénbreen has been determined using a combination of surface mapping and ground-penetrating radar, and consists of: (1) folding of primary stratification together with supraglacially derived debris, together with the development of an axial plane longitudinal foliation; (2) intersecting sets of crevasse traces; (3) development of arcuate upglacier-dipping fractures as part of a thrust complex near the snout, and (4) formation of longitudinal splaying fractures in the snout area.

[69] 2. A numerical modeling experiment, which generates a cumulative strain pattern for most of the glacier surface, successfully explains the origin of most structures. Longitudinal foliation forms under a simple shear regime that is strongest near flow unit boundaries. Folded stratification broadly mirrors the long axes of strain ellipses between flow unit boundaries. Fractures near the snout, interpreted as thrusts, clearly form in a longitudinal compressive flow regime.

[70] 3. Crevasse traces and thrusts appear are no longer actively forming. They are interpreted as relict, formed during the Neoglacial maximum when the ice was more dynamic and moving over soft, wet sediment that underlay much of the lower glacier. Nevertheless, the strain-ellipse pattern (with long axes of ellipses parallel to thrusts) is conducive for renewed thrusting if basal conditions once again became favorable.

[71] 4. During the 20th century, as the glacier receded and thinned, the ratio of wet to frozen bed has decreased, as indicated by the changing structural regime.

[72] 5. As recession continues into the future, the glacier is likely to become frozen to the bed throughout and near-stagnant; structural evolution will then almost cease, a situation that already prevails at nearby austre Brøggerbreen.

[73] **Acknowledgments.** This research was funded by a U.K. Natural Environment Research Council grant (GST/022192) under the ARCICE Thematic Programme. We thank Nick Cox, Brian Hansen, and Martin Davey at the NERC Arctic Research Station in Ny-Ålesund for logistical support and Jon-Ove Hagen (University of Oslo), Jemma Wadham (University of Bristol), and Adrian Luckman (University of Wales, Swansea) for useful discussions concerning the glacier. The GPR fieldwork was undertaken with ample assistance from Andy Smith and Ed King (British Antarctic Survey) and Bernd Kulessa (Queen's University, Belfast). We thank Robert Anderson and Garry Clarke for their constructive comments on the manuscript.

References

Albrecht, O., P. Jansson, and H. Blatter (2000), Modelling glacier response to measured climate forcing, *Ann. Glaciol.*, *31*, 91–96.

Allen, C. R., W. B. Kamb, M. F. Meier, and R. P. Sharp (1960), Structure of the lower Blue Glacier, Washington, *J. Geol.*, *68*, 601–625.

Björnsson, H., Y. Gjessing, S. E. Hamran, J. O. Hagen, O. Liestøl, F. Pálsson, and B. Erlingsson (1996), The thermal regime of sub-polar glaciers mapped by multi-frequency radio-echo sounding, *J. Glaciol.*, *42*, 23–32.

Blatter, H. (1995), Velocity and stress fields in grounded glaciers: A simple algorithm for including deviatoric stress gradients, *J. Glaciol.*, *41*, 333–343.

Clarke, G. K. C., and E. W. Blake (1991), Geometric and thermal evolution of a surge-type glacier in its quiescent state: Trapridge Glacier 1969–1989, *J. Glaciol.*, *37*, 158–169.

De Geer, G. (1930), Flygfärder och polarforskning från Andrée till nutiden, *Jorden Runt*, *2*, 577–608.

Dowdeswell, J. A., R. Hodgkins, A.-M. Nuttall, J. O. Hagen, and G. S. Hamilton (1995), Mass balance change as a control on the frequency and occurrence of glacier surges in Svalbard, Norwegian High Arctic, *Geophys. Res. Lett.*, *22*, 2909–2912.

Dowdeswell, J. A., et al. (1997), The mass balance of circum-arctic glaciers and recent climate change, *Quat. Res.*, *48*, 1–14.

Durney, D. W., and J. G. Ramsay (1973), Incremental strain measured by syntectonic crystal growth, in *Gravity and Tectonics*, edited by K. A. Jong and R. Scholten, pp. 67–96, John Wiley, Hoboken, N. J.

Fleming, K. M., J. A. Dowdeswell, and J. Oerlemans (1997), Modelling the mass balance of northwest Spitsbergen glaciers and responses to climate change, *Ann. Glaciol.*, *24*, 203–210.

Glasser, N. F., and M. J. Hambrey (2001), Styles of sedimentation beneath Svalbard valley glaciers under changing dynamic and thermal regimes, *J. Geol. Soc.*, *158*, 697–707.

Glasser, N. F., M. J. Hambrey, K. Crawford, M. R. Bennett, and D. Huddart (1998), The structural glaciology of Kongsvegen, Svalbard and its role in landform genesis, *J. Glaciol.*, *44*, 136–148.

Glasser, N. F., M. J. Hambrey, J. L. Etienne, P. Jansson, and R. Pettersson (2003), The origin and significance of debris-charged ridges at the surface of Storglaciären, northern Sweden, *Geogr. Ann.*, *85A*, 127–147.

Goodsell, B. C., M. J. Hambrey, and N. F. Glasser (2002), Formation of ogives and associated structures on the Bas Glacier d'Arolla, Valais, Switzerland, *J. Glaciol.*, *48*, 287–300.

Goodsell, B. C., M. J. Hambrey, N. F. Glasser, P. Nienow, and D. Mair (2005), The structural glaciology of a temperate valley glacier: Haut Glacier d'Arolla, Valais, Switzerland, *Arct. Antarct. Alp. Res.*, in press.

Hagen, J. O., and O. Liestøl (1990), Long term glacier mass balance investigations in Svalbard 1950–88, *Ann. Glaciol.*, *14*, 102–106.

Hagen, J. O., and A. Sætrang (1991), Radio-echo soundings of sub-polar glaciers with low-frequency radar, *Pol. Res.*, *26*, 15–57.

Hagen, J. O., O. M. Korsen, and G. Vatne (1991), Drainage pattern in a subpolar glacier: Brøggerbreen, Svalbard, in *Arctic Hydrology: Present and Future Tasks*, edited by Y. Gjessing et al., *Rep. 23*, 141 pp., Norw. Natl. Comm. for Hydrol., Oslo.

Hagen, J. O., O. Liestøl, E. Roland, and T. Jørgensen (1993), *Glacier Atlas of Svalbard and Jan Mayen*, Norsk Polarinst. Medd., Oslo.

Hagen, J. O., K. Melvold, F. Pinglot, and J. A. Dowdeswell (2003), On the net mass balance of the glaciers and ice caps in Svalbard, Norwegian Arctic, *Arct. Antarct. Alp. Res.*, *35*, 264–270.

Hamberg, A. (1894), En resa til norra Ishafet sommaren 1892, *Ymer*, *14*, 25–61.

Hambrey, M. J. (1977), Foliation, minor folds and strain in glacier ice, *Tectonophysics*, *39*, 397–416.

Hambrey, M. J., and J. A. Dowdeswell (1997), Structural evolution of a surge-type glacier: Hessbreen, Svalbard, *Ann. Glaciol.*, *24*, 375–381.

Hambrey, M. J., and N. F. Glasser (2003), The role of folding and foliation development in the genesis of medial moraines: Examples from Svalbard glaciers, *J. Geol.*, *111*, 471–485.

Hambrey, M. J., and W. L. Lawson (2000), Structural styles and deformation fields in glaciers: A review, *Spec. Publ. Geol. Soc. London*, *176*, 59–83.

Hambrey, M. J., and A. G. Milnes (1977), Structural geology of an Alpine glacier (Griesgletscher, Valais, Switzerland), *Ecol. Geol. Helv.*, *70*, 667–684.

Hambrey, M. J., and F. Müller (1978), Structures and ice deformation in the White Glacier, Axel Heiberg Island, Northwest Territories, Canada, *J. Glaciol.*, *20*, 41–66.

Hambrey, M. J., J. A. Dowdeswell, T. Murray, and P. R. Porter (1996), Thrusting and debris-entrainment in a surging glacier, Bakaninbreen, Svalbard, *Ann. Glaciol.*, *22*, 241–248.

Hambrey, M. J., D. Huddart, M. R. Bennett, and N. F. Glasser (1997), Dynamic and climatic significance of "hummocky moraines": Evidence from Svalbard and Britain, *J. Geol. Soc.*, *154*, 623–632.

Hambrey, M. J., M. R. Bennett, J. A. Dowdeswell, N. F. Glasser, and D. Huddart (1999), Debris entrainment and transfer in polythermal valley glaciers, *J. Glaciol.*, *45*, 69–86.

Hansen, S. (1999), A photogrammetrical, climate-statistical and geomorphological approach to the post Little Ice Age changes of the Midre Lovénbreen glacier, Svalbard, M.S. thesis, 84 pp., Dept. of Phys. Geogr., Univ. of Copenhagen.

Hansen, S. (2003), From surge-type to non-surge type glacier behaviour: Midre Lovenbreen, Svalbard, *Ann. Glaciol.*, *36*, 97–102.

Hodson, A. J., M. Tranter, J. A. Dowdeswell, A. M. Gurnell, and J. O. Hagen (1997), Glacier thermal regime and suspended-sediment yield: A comparison of two high-Arctic glaciers, *Ann. Glaciol.*, *24*, 32–37.

Hooke, R. L., and P. J. Hudleston (1978), Origin of foliation in glaciers, *J. Glaciol.*, *20*, 285–299.

Hubbard, A., and B. Hubbard (2000), The potential contribution of high-resolution glacier flow modelling to structural glaciology, *Spec. Publ. Geol. Soc. London*, *176*, 135–146.

Hubbard, A., H. Blatter, P. Nienow, D. Mair, and B. Hubbard (1998), Comparison of a three-dimensional model for glacier flow with field data from Haut Glacier d'Arolla, Switzerland, *J. Glaciol.*, *44*, 368–378.

Hubbard, A., W. Lawson, B. Anderson, B. Hubbard, and H. Blatter (2005), Evidence for subglacial ponding across Taylor Glacier, Dry Valleys, Antarctica, *Ann. Glaciol.*, in press.

Isachsen, G. (1912), Résultats des campagnes scientifiques accomplies sur son yacht par Albert ler, Prince Souverain de Monaco, in *Exploration du nord-ouest du Spitsberg enterprise sous les auspices de S. A. S. le Prince de Monaco par la mission Isachsen*, vol. 1, *Rep. 40*, Christiania, Monaco.

Janssen, P., J.-O. Näslund, R. Pettersson, C. Richardson-Näslund, and P. Holmlund (2000), Debris entrainment and polythermal structure in the terminus of Storglaciären, *IASH Publ.*, *264*, 143–151.

Jiskoot, H., T. Murray, and P. J. Boyle (2000), Controls on the distribution of surge-type glaciers in Svalbard, *J. Glaciol.*, *46*, 412–422.

Lawson, W. (1996), Structural evolution of Variegated Glacier, Alaska, USA, since 1948, *J. Glaciol.*, *42*, 261–270.

Lefauconnier, B., and J. O. Hagen (1990), Glaciers and climate in Svalbard: Statistical analysis and reconstruction of the Brøgger Glacier mass balance for the last 77 years, *Ann. Glaciol.*, *14*, 148–152.

Liestøl, O. (1988), The glaciers in the Kongsfjorden area, Spitsbergen, *Norsk Geogr. Tids.*, *42*, 231–238.

Meier, M. F. (1960), Mode of flow of Saskatchewan Glacier, Alberta, Canada, *U.S. Geol. Surv. Prof. Pap., 351*, 70 pp.

Murray, T., D. L. Gooch, and G. W. Stuart (1997), Structures within the surge front at Bakaninbreen, Svalbard, using ground-penetrating radar, *Ann. Glaciol.*, *24*, 122–129.

Murray, T., G. W. Stuart, P. J. Miller, J. Woodward, A. M. Smith, P. R. Porter, and H. Jiskoot (2000), Glacier surge propagation by thermal evolution at the bed, *J. Geophys. Res.*, *105*, 13,491–13,507.

Ødegård, R. S., S.-E. Hamran, P. H. Bø, B. Etzelmüller, G. Vatne, and J. L. Sollid (1992), Thermal regime of a valley glacier, Erikbreen, northern Spitsbergen, *Pol. Res.*, *2*, 69–79.

Post, A., and E. R. LaChapelle (1971), *Glacier Ice*, Univ. of Wash. Press, Seattle.

Ramsay, J. G., and M. Huber (1983), *The Techniques of Modern Structural Geology*, vol. 1, *Strain Analysis*, 307 pp., Elsevier, New York.

Rippin, D., I. Willis, N. Arnold, A. Hodson, J. Moore, J. Kohler, and H. Björnsson (2003), Changes in geometry and subglacial drainage of Midre Lovénbreen, Svalbard, determined from digital elevation models, *Earth Surf. Processes Landforms*, *28*, 273–298.

Schneeberger, C., O. Albrecht, H. Blatter, M. Wild, and R. Hock (2001), Modelling the response of glaciers to a doubling of atmospheric CO_2: A case study of Storglaciären, northern Sweden, *Clim. Dyn.*, *17*, 825–834.

Wadham, J. L., and A.-M. Nuttall (2003), Multiphase formation of superimposed ice during a mass-balance year at a maritime high-Arctic glacier, *J. Glaciol.*, *48*, 545–551.

Woodward, J., T. Murray, and A. McCaig (2002), Formation and reorientation of structures in the surge-type glacier Kongsvegen, Svalbard, *J. Quat. Sci.*, *17*, 201–209.

N. F. Glasser, M. J. Hambrey, and B. Hubbard, Centre for Glaciology, Institute of Geography and Earth Sciences, University of Wales, Aberystwyth, Ceredigion SY23 3DB, UK. (nfg@aber.ac.uk; mjh@aber.ac.uk; byh@aber.ac.uk)

S. Hansen, Institute of Geography, University of Copenhagen, Øster Voldgade 10, DK-1350 Copenhagen, Denmark. (sh@geogr.ku.dk)

A. Hubbard, Department of Geography, University of Edinburgh, Drummond Street, Edinburgh EH8 9XP, UK. (alh@tsunami.geo.ed.ac.uk)

J. Kohler, Norwegian Polar Institute, Polar Environmental Centre, N-9296 Tromsø, Norway. (jack.kohler@npolar.no)

T. Murray, School of Geography, University of Leeds, Leeds LS2 9JT, UK. (t.murray@geog.leeds.ac.uk)

G. Stuart, School of Earth Sciences, University of Leeds, Leeds LS2 9JT, UK. (g.stuart@earth.leeds.ac.uk)